

Modeling the airflow in a lung with cystic fibrosis

Sara Zarei, Ali Mirtar, Bjarne Andresen and
Peter Salamon

Keywords. Cystic fibrosis (CF), spirometry, lung air flow, airway resistance in lungs.

Abstract

Cystic fibrosis (CF) is a chronic progressive pulmonary disorder caused by mutations in the CFTR (cystic fibrosis transmembrane conductance regulator) gene. A CF lung is generally characterized by obstructed airflow to an extent that leads to destruction of airway wall support structure. Airway resistance, resulting from both laminar and turbulent flow, is an important mechanical factor contributing to flow of air into and out of the airways. There are numerous research studies focusing on airflow in the respiratory system that assumed flow to be only laminar and steady. The goal of this research is to describe the air flow mathematically by considering the resistance from both laminar and turbulent airflow throughout the entire respiratory tract. Furthermore, we implement a model that includes airway clogging in CF lungs and recalculate the rate of air flow given these obstructions.

1 Introduction


Pulmonologists and general practice physicians commonly use spirometry tests when evaluating and managing pulmonary obstruction diseases. Spirometry is a basic pulmonary function test that is widely used for the detection of airflow impediments and limitations. The test measures volumes of air during inhalation and exhalation maneuvers as a function of time. Two of the most important test values of spirometry are FEV₁, forced expiratory volume in one second, and FVC, forced vital capacity. (FVC, forced vital capacity, is a spirometric test that measures volume of air that can forcibly be blown out after a full inspiration maneuver.)

There have been numerous studies describing the physiological basis of forced expiration and spirometry test results. Most of them assumed the lung airways to be a system of smooth adjoined cylinders through which air flows in a laminar fashion and their results are based on the assumption of the steady flow [6, 7, 26]. This assumption completely ignores the turbulent flow in upper airways and thus is insufficient for predicting physiologically realistic transport of particles by the airflow. Therefore, current computational and experimental models are unable to assess the flow through the entire lung airways [23]. A proper airway flow model needs to consider the nature of airflow as it occurs throughout the entire respiratory tract. In this paper we propose a mathematical model that can calculate the rate of airflow as well as the total resistance in a CF lung. For our modeling purposes we assume a rigid airway tree structure and consider turbulent as well as transitional and laminar flow through this structure. The different flux–force relationships in the different regions combined with the 2^{23} segments of the airway make this a challenging but doable problem.

Our main goal however is not the prediction of flow through the unobstructed airway. Rather, it is flow through the partially obstructed airways of a CF lung that is our main concern. In this regard, the present work is built upon and further tests our previous model for mucus presence in a CF lung [27]. That model follows the location and growth of pockets of mucus; its parameters were estimated using mean FVC data as a function of age for patients at the University of California San Diego Adult Cystic Fibrosis Center. The model identified several interesting parameters such as probability of colonization, mucus volume growth rate, and scarring rate. In the present work we calculate predicted average FEV1 values for this population, enabling a stronger test of our mucus distribution model.

We go on to apply our model to predict FVC and FEV1 for more hypothetical distributions. This enables us to understand the effects of degrees of spreading or localization in pockets of infection. Thus we examine trends in FEV1 values as we redistribute a given volume of mucus different ways.

The measurement of airflow and airway resistance has received considerable attention in respiratory physiology. Patients with cystic fibrosis experience a progressive decline in pulmonary function over the course of the disease. This decline can be shown by monitoring forced expiratory volume in 1 s (FEV1) [4, 5, 13]. This indicates the need for understanding the relationship between airway structure, airflow, and airway resistance in a CF lung. A mathematical model that describes such a relationship can be used to improve diagnosis and treatment of the disease.



Generation (n)	Number (2 ⁿ)	Diameter (cm)	Length (cm)	Total cross-sectional area (cm) ²	Total volume (cm) ³	Total resistance (Pa.s/m ³)	
Trachea	0	1	1.80	12	2.54	30.54	911.88
Bronchi	1	2	1.22	4.76	2.34	11.18	860.61
	2	4	0.83	1.900	2.16	4.11	798.41
	3	8	0.56	0.76	1.97	1.50	770.58
	4	16	0.45	1.27	2.54	3.23	1,544.12
Bronchioles	5	32	0.35	1.07	3.08	3.29	1,777.49
	Terminal bronchiole	16	65,536	0.049	0.112	123.58	13.84
Respiratory bronchioles	17	↓	↓	↓	↓	↓	↓
	18	524,288	0.036	0.070	533.66	37.36	63.41
Alveolar ducts	19	↓	↓	↓	↓	↓	↓
	20	↓	↓	↓	↓	↓	↓
	21	4,194,304	0.029	0.067	2,770.42	185.62	18.02
Alveolar sacs	22	8,388,608	0.025	0.075	4,117.74	308.83	18.26

Figure 1. Dichotomous branching of airways in the human lung. (Source: Adapted from Ref. [25])

2 Different flow types in human respiratory system

The human respiratory system can be described as a tree that starts at the trachea and bifurcates 23 times before reaching the alveolar sacs [14, 25]. We will refer to each bifurcation as one generation in the lung. Figure 1 provides the corresponding measurements of each airway generation such as diameter, length, total cross section, etc.¹ In order to calculate the rate of air flow in a CF lung, we first need to identify the corresponding flow type existing within different generations of a lung’s airways. Turbulent flow occurs when air is flowing through an airway at a high velocity. This results in production of chaotic flow along with the formation of eddies.

In human lungs turbulent flow is found mainly in the larger airways like the trachea, while laminar flow involves low velocities and is found in the

¹ These measurements were obtained directly from the Weibel lung model [25]. We believe the corresponding length of the third generation should be 1.76 instead of 0.76 cm, in keeping with the general trend in airway sizes of other generations.

smaller tubes called bronchioles. Laminar flow tends to be more orderly and streamlined than turbulent flow. During quiet breathing, laminar flow exists from the medium-sized bronchi down to the bronchiole levels. Transitional flow, which has some of the characteristics of both laminar and turbulent flow, is found between the two along the bronchial tree [1].

The Reynolds number (R_e) is commonly used to identify the different types of flow. We used R_e in our simulation to determine the type of flow that exists within each airway. R_e is a dimensionless parameter that measures the ratio of inertial forces to viscous forces [10, 20, 24]. For flow through a pipe of diameter d ,

$$R_e = \frac{\rho V^2}{\frac{\mu \cdot V}{d}} = \frac{Vd}{\nu} \quad (1)$$

where ρ is the fluid density [$1.2 \text{ kg}\cdot\text{m}^{-3}$], V is the mean linear velocity of the fluid [m/s], μ is the fluid viscosity [$1.958 \cdot 10^{-5} \text{ Pa}\cdot\text{s}$], and $\nu = \frac{\mu}{\rho}$ is the kinematic viscosity [m^2/s] (the values are for humid air).

The volume rate of flow, ϕ , is

$$\phi = V \cdot A, \quad (2)$$

where A is the pipe's cross-sectional area. Using Eqs. (1) and (2) we can rewrite the Reynolds number in terms of the flow rate:

$$R_e = \frac{2\rho\phi}{\pi r\mu}, \quad (3)$$

where r is the radius of the pipe.

Using Eq. (3) we found the average Reynolds number for each of the 23 different airway generations. In our calculation we used the corresponding value of air density and viscosity at the human body temperature. In addition, we utilized the average airflow of an adult lung, 4–5 l/s, for the ϕ substitution in Eq. (3). In order to group different generations of lung based on their flow type, we utilized the following ranges of the Reynolds numbers [8]:



There are different empirical definitions of the ranges for the laminar, transitional, and turbulent flow. For our research, we chose 2300/4000 as the switching points while, e.g., Moody picked 640/5000 [21].

Generation #	Reynolds #	Air flow type
1	17706	Turbulent
2	13061	Turbulent
3	9599	Turbulent
4	7114	Turbulent
5	4426	Turbulent
6	2845	Transitional
7	1778	Laminar
8	1082	Laminar
..., 23	< 1000	Laminar

Table 1. Reynolds number result.

Based on our result for a healthy lung, the first five airway lung generations have turbulent flow, the sixth generation has transitional flow, and the rest carry laminar flow. This is in agreement with Ref. [21]. The results are shown in Table 1.

3 All-laminar lung model

For simplicity, many studies assume that all 23 generations of lung airways have laminar flow [3, 15, 19, 28]. In this section first we use this assumption to calculate the rate of airflow in the respiratory system. This will show the necessity of including the turbulent flow when calculating airflow or resistance of lung airways. It also proves useful as a way to calculate laminar flow in the higher generation airways, even after we transition to mixed flow types.

By considering that all respiratory airways carry only laminar flow, we can use Poiseuille's law of fluid dynamics to calculate the resistance of each generation. This law states that in a laminar flow, ϕ is proportional to the pressure difference, ΔP , between the ends of the pipe and the fourth power of the radius $r = \frac{d}{2}$ [2, 18, 22].

$$\Delta P = \frac{8 \cdot \mu \cdot L \cdot \phi}{\pi \cdot \left(\frac{d}{2}\right)^4}, \quad (4)$$

where ΔP is the pressure drop and L is the length of the pipe. The resis-

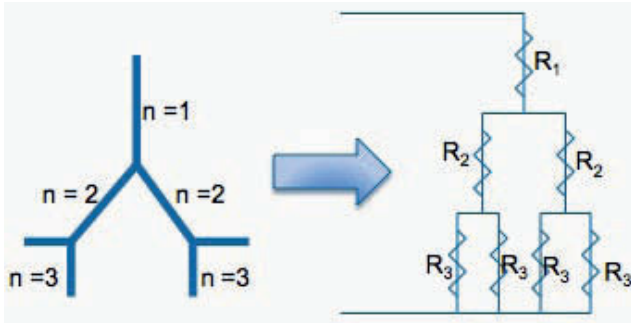


Figure 2. Airway resistance model assuming laminar flow for a tree with three generations. R_i represents the corresponding resistance in each generation. Due to the symmetry of the circuit, each bronchiole has the same resistance as other bronchioles within the same generation.

tance (R) in Poiseuille flow is

$$R = \frac{8 \cdot \mu \cdot L}{\pi \cdot \left(\frac{d}{2}\right)^4}. \quad (5)$$

Note that the effective resistance in a tube is inversely proportional to the fourth power of the radius. This means that halving the radius of the tube, due to (say) mucus production in a CF lung, can increase the resistance to airflow by a factor of 16. We calculate the total resistance by considering the series and parallel circuits that the branching airways form. Due to the symmetric structure of the circuit (see Figure 2), the two nodes connecting R_2 s to R_3 s have the same potential and thus we can consider them connected. The four R_3 resistors in parallel have a combined resistance of $\frac{R_3}{4}$. Hence the total resistance is

$$R_{\text{Total}} = (R_1) + \left(\frac{R_2}{2}\right) + \left(\frac{R_3}{4}\right) + \left(\frac{R_4}{8}\right) + \dots + \left(\frac{R_n}{2^{n-1}}\right) + \dots + \left(\frac{R_{23}}{2^{22}}\right). \quad (6)$$

Using Eqs. (4), (5), and (6), we calculated the corresponding air flow of a normal healthy lung based on a ΔP of 45 cm H_2O [12]. The resulting flow is 1056 l/s. This quantity of airflow is unrealistically high for a human respiratory system. This is due to neglecting the extra resistance as the result of turbulent flow in the upper airways. While a single small airway provides more resistance than a single large airway, resistance to air flow depends on the number of parallel pathways present. For this reason, the large and particularly the medium-sized airways actually provide greater resistance to flow than do the more numerous small airways. For turbulent

flow, resistance is relatively large. That is, compared with laminar flow, a much larger driving pressure is required to produce the same flow rate. Because the pressure–flow relationship ceases to be linear during turbulent flow, no simple equation exists to compute resistance. Therefore in the next section we construct a system of equations using the pressure–flow relationship in transitional and turbulent flow to calculate FEV1 and total lung resistance.

4 Turbulent and transitional airflow in a lung

In any network of rigid tubes (e.g., human respiratory airways), the pressure drop between two points can be attributed to two reasons. The first is due to the changes in kinetic energy as the fluid accelerates or decelerates (Bernoulli effect). The second is due to dissipation of energy as a result of viscosity [11, 17]. Under steady or quasi-steady flow conditions, the ratio of pressure loss due to viscosity to the kinetic energy per unit volume is called the coefficient of friction or friction factor, which is a dimensionless quantity [9, 17].

The friction coefficient (C_F) is defined as

$$C_F = \frac{2\Delta P}{\rho V^2}. \quad (7)$$

From Eq. (7) we have

$$\Delta P = \frac{1}{2} C_F \rho V^2.$$

To build a model that calculates FEV1, we used the Moody diagram in Figure 3. The Moody diagram illustrates the relationship between Reynolds number (R_e) and friction coefficient (C_F) in a network of branched tubes similar to human airways [21]. Figure 3 shows the friction coefficient (C_F) against Reynolds number (R_e) in a log-log plot:

$$C_F = a \cdot R_e^b.$$

Based on this figure we have three different linear relationships between a power of the Reynolds number and the friction coefficient. They correspond to the functional form in laminar, transitional, and turbulent flow. We continue using Poiseuille's law for laminar flow, while we use the Moody diagram for the other two flow types.

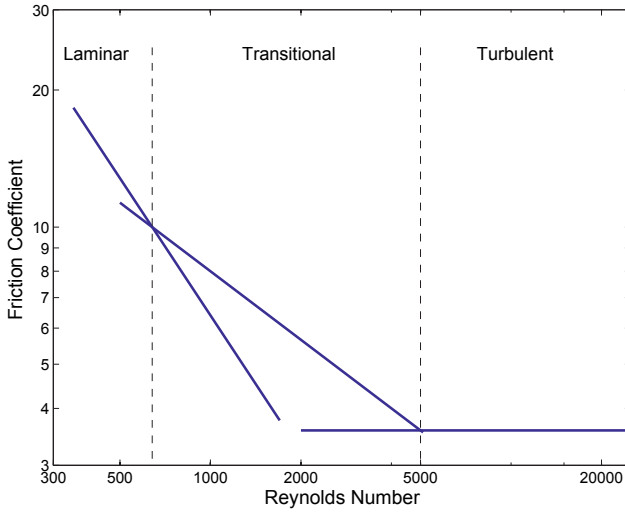


Figure 3. Moody plot of friction coefficient (C_f) against tracheal Reynolds numbers (R_e) for inspiratory flow in airways of human bronchial tree. Solid lines have slopes of -1 , $-1/2$, and 0 . (Source: Adapted from [21])

For the transitional flow, $640 \leq R_e \leq 5000$, we have

$$\Delta P = 40 \sqrt{\frac{10\mu\rho V^3}{d}} = 40 \sqrt{\frac{10\mu\rho}{A^3 \cdot d}} \cdot \phi^{\frac{3}{2}} = K_0 \cdot \phi^{\frac{3}{2}}, \quad (8)$$

where $K_0 = 40 \sqrt{\frac{10\mu\rho}{A^3 \cdot d}}$.

For turbulent flow, where $R_e \geq 5000$, we have

$$\Delta P = \frac{4}{\sqrt{5}} \rho V^2 = \frac{4\rho}{\sqrt{5}A^2} \phi^2 = K \cdot \phi^2, \quad (9)$$

where $K = \frac{4\rho}{\sqrt{5}A^2}$. Using the airway dimensions in the first five generations of a lung, we can get the corresponding turbulent flow coefficient K values in $\frac{\text{kg}}{\text{s} \cdot \text{m}^4}$. The K values are given by

$$\begin{aligned} K_1 &= 3.32 \cdot 10^7 \frac{\text{kg}}{\text{s} \cdot \text{m}^4}, & K_2 &= 1.57 \cdot 10^8 \frac{\text{kg}}{\text{s} \cdot \text{m}^4}, \\ K_3 &= 7.33 \cdot 10^8 \frac{\text{kg}}{\text{s} \cdot \text{m}^4}, & K_4 &= 3.54 \cdot 10^9 \frac{\text{kg}}{\text{s} \cdot \text{m}^4}. \end{aligned}$$

In the next section we demonstrate how we implemented this process computationally, in order to calculate the rate of airflow or FEV1 in a CF lung.

5 The FEV1 calculation

Kirchhoff's current law derives from the principle of conservation of electric charge in a circuit. It states that at any node or junction in an electrical circuit, the sum of currents flowing into that node is equal to the sum of currents flowing out of that node. In other words, the algebraic sum of currents in a network of conductors meeting at a point is zero [16]. By considering the trachea as the beginning of this circuit's node and the bronchioles located on generation 23 as our end node, we can construct the following system of equations that expresses the relationship between airflow, resistance, and pressure drop. For display purposes, we assume only the first two generations are turbulent, one is transitional, and the rest are laminar. In our simulation we considered the first five bifurcations with turbulent flow. Thus we have the following system of equations:

$$\begin{aligned}
 \text{(I)} \quad & \phi_1 = \phi_2 + \phi_3, \\
 \text{(II)} \quad & \phi_2 = \phi_4 + \phi_5, \\
 \text{(III)} \quad & \phi_3 = \phi_6 + \phi_7, \\
 \text{(IV)} \quad & \Delta P = \phi_1^2 \cdot K_1 + \phi_2^2 \cdot K_2 + \phi_4^{\frac{3}{2}} \cdot K_4 + \phi_4 \cdot R_4, \\
 \text{(V)} \quad & \Delta P = \phi_1^2 \cdot K_1 + \phi_2^2 \cdot K_2 + \phi_5^{\frac{3}{2}} \cdot K_5 + \phi_5 \cdot R_5, \\
 \text{(VI)} \quad & \Delta P = \phi_1^2 \cdot K_1 + \phi_3^2 \cdot K_3 + \phi_6^{\frac{3}{2}} \cdot K_6 + \phi_6 \cdot R_6, \\
 \text{(VII)} \quad & \Delta P = \phi_1^2 \cdot K_1 + \phi_3^2 \cdot K_3 + \phi_7^{\frac{3}{2}} \cdot K_7 + \phi_7 \cdot R_7,
 \end{aligned} \tag{10}$$

where ΔP is the pressure drop across the airways (assuming all alveoli are at the same pressure), ϕ_n are the airflow rates, R_n are laminar resistance from smaller airways: generations 4 to 23, and K_n are the turbulent or transitional flow coefficient constants.

As you can infer, the symmetry of the bronchial tree was not used in Eq. (10) as it was used in Eq. (6). This is due to the fact that a CF patient's lung has obstructive bronchioles, therefore the airways are no longer symmetric.

Figure 4 illustrates the layout of this system. As shown in this figure ϕ_1 , ϕ_2 , and ϕ_3 represent the turbulent flows and ϕ_4 , ϕ_5 , ϕ_6 , and ϕ_7 are the transitional flows. Since these transitional flows enter the laminar region, the pressure drop in this region is calculated by multiplying the flow by the total resistance of the laminar section under the corresponding subtree. To solve the system of equations shown above, first we rewrite the system into

matrix format. Using Kirchhoff's current law (KCL) we can rewrite the first three equations of system (10) as follows:

$$\underbrace{\begin{bmatrix} 1 & -1 & -1 & 0 & 0 & 0 & 0 \\ 0 & 1 & 0 & -1 & -1 & 0 & 0 \\ 0 & 0 & 1 & 0 & 0 & -1 & -1 \end{bmatrix}}_{F_1} \times \underbrace{\begin{bmatrix} \phi_1 \\ \phi_2 \\ \phi_3 \\ \phi_4 \\ \phi_5 \\ \phi_6 \\ \phi_7 \end{bmatrix}}_{\Phi} = \begin{bmatrix} 0 \\ 0 \\ 0 \end{bmatrix}. \quad (11)$$

Next, we rewrite Kirchhoff's voltage law (KVL) of equations (IV)–(VII) in system (10) into a matrix format:

$$F_2 \times \underbrace{\begin{pmatrix} \phi_1^2 \\ \phi_1^{\frac{3}{2}} \\ \phi_1 \\ \phi_2^2 \\ \phi_2^{\frac{3}{2}} \\ \phi_2 \\ \vdots \\ \phi_7 \end{pmatrix}}_{\hat{\Phi}} = \begin{pmatrix} \Delta P \\ \Delta P \\ \Delta P \\ \Delta P \end{pmatrix}, \quad (12)$$

where F_2 is

$$\begin{pmatrix} K_1 & 0 & 0 & K_2 & 0 & 0 & 0 & 0 & 0 & 0 & K_4 & R_4 & 0 & 0 & 0 & 0 & 0 & 0 & 0 & 0 \\ K_1 & 0 & 0 & K_2 & 0 & 0 & 0 & 0 & 0 & 0 & 0 & 0 & 0 & 0 & K_5 & R_5 & 0 & 0 & 0 & 0 & 0 \\ K_1 & 0 & 0 & 0 & 0 & 0 & K_3 & 0 & 0 & 0 & 0 & 0 & 0 & 0 & 0 & 0 & K_6 & R_6 & 0 & 0 & 0 \\ K_1 & 0 & 0 & 0 & 0 & 0 & K_3 & 0 & 0 & 0 & 0 & 0 & 0 & 0 & 0 & 0 & 0 & 0 & 0 & K_7 & R_7 \end{pmatrix}$$

We expanded the columns of matrix F_1 from Eq. (11) to be the same size as the number of columns of matrix F_2 from Eq. (12). This was done by adding two leading zero columns before each entry in matrix F_1 . Assume

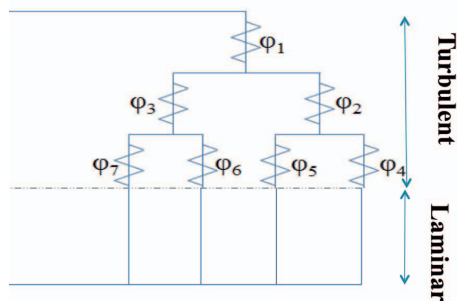


Figure 4. Airway resistance model using laminar, transitional, and turbulent flows. For display purposes, we are only assuming the first two generations to carry turbulent flow, the third generation to have transitional flow, and the rest to have laminar flow. ϕ_i represents the amount of airflow in bronchiole i .

F_1 is an $m \times n$ matrix, then each element of the new matrix, \widehat{F}_1 , can be described as follows:

$$\widehat{F}_1(i, j) = \begin{cases} F_1(i, \frac{j}{3}) & \text{if } j \bmod 3 = 0, \\ 0 & \text{if } j \bmod 3 \neq 0, \end{cases} \tag{13}$$

where $1 \leq i \leq m, 1 \leq j \leq 3n$.

Furthermore, matrix Φ from Eq. (11) is an $m \times 1$ vector. We can describe elements of $\widehat{\Phi}$ from Eq. (12) as follows:

$$\widehat{\Phi}(j) = \begin{cases} \Phi^2(\lceil \frac{j}{3} \rceil) & \text{if } j \bmod 3 = 1, \\ \Phi^{\frac{3}{2}}(\lceil \frac{j}{3} \rceil) & \text{if } j \bmod 3 = 2, \\ \Phi(\lceil \frac{j}{3} \rceil) & \text{if } j \bmod 3 = 0. \end{cases} \tag{14}$$

Based on the statement in Eqs. (13) and (14), we get

$$F_1 \Phi = \widehat{F}_1 \widehat{\Phi}_1.$$

To rewrite the entire Eq. (10) into matrices, first we define matrix M :

$$M = \begin{bmatrix} \widehat{F}_1 \\ F_2 \end{bmatrix}.$$

Finally, in order to identify the FEV1, we need to solve the following equation in such a way that we get a vector of zeros for the residual value.

Note that the first entry in matrix Φ represents the FEV1 value.

$$\text{Residual} = M \cdot [\hat{\Phi}] - \begin{bmatrix} 0 \\ \vdots \\ 0 \\ \Delta p \\ \vdots \\ \Delta p \end{bmatrix}. \quad (15)$$

In matrix (15)

number of zeros = number of rows in matrix F_1

and

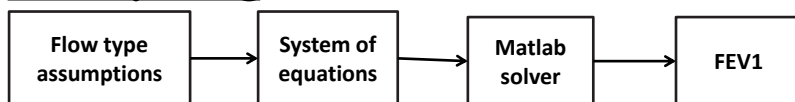
numbers of ΔP 's = number of rows in matrix F_2 .

Also, based on the maximum forced expiratory maneuvers experiment that was conducted by Ref. [12], the average pressure drop in a human lung was determined to be approximately 45 cm H_2O . Using our turbulent and transitional model on average, a healthy lung airflow is 4.5 l/s for $\Delta P = 45$ cm H_2O .

Figure 5 displays the process of calculating the FEV1 for both healthy and CF lungs. For the healthy lung, we start with our initial assumptions of flow type within different lung generations as depicted in Table 1. On the other hand, since flow type will change as a tube is filled with mucus, we always need to check the Reynolds number after each iteration. Therefore, in a normal healthy lung, we can solve Eq. (15) for FEV1 or (ϕ_1), without modifying any of the variables. But due to the obstruction of airways in a CF lung, the effective diameter of bronchioles will vary once infected. Hence, in order to calculate the final rate of airflow (FEV1) in a CF lung, we will need to recheck the Reynolds number of each tube to check for any changes that were made due to mucus production.

At each iteration we first find the number of variables to construct the equations and the matrix F_1 . A preponderance of computational details are eschewed so that important concepts can be highlighted. Once we locate all required variables, we next determine the corresponding coefficient values as previously explained in Eqs. (8) and (9). At this stage we are also required to find the total resistance of those bronchioles that have laminar flow. Next we use the depth-first traversal algorithm to travel through this

Healthy Lung



CF Lung

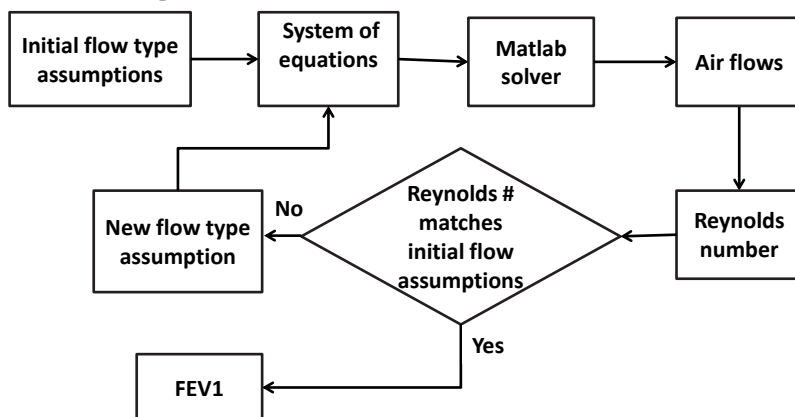


Figure 5. FEV1 calculation process flowchart for healthy and CF lung.

binary tree from the trachea all the way down to the first laminar generation. Therefore, we visit every possible path from trachea to the first laminar bronchiole and construct the matrix F_2 . Finally, after setting up the equations, we use Matlab's `fsolve` to identify the corresponding FEV1 value.

6 Results

In this section we evaluate our proposed airflow model by comparing its predictions for average FEV1 values based on mucus distributions obtained in Ref. [27]. We end the section by discussing the effects of spreading and partial filling on FEV1 values.

6.1 Predicted mean FEV1 values

In our previous paper [27], we proposed a model that quantitatively characterized the distribution of mucus in the CF patient's respiratory airways as a function of time. The parameters in the model were fitted to the average

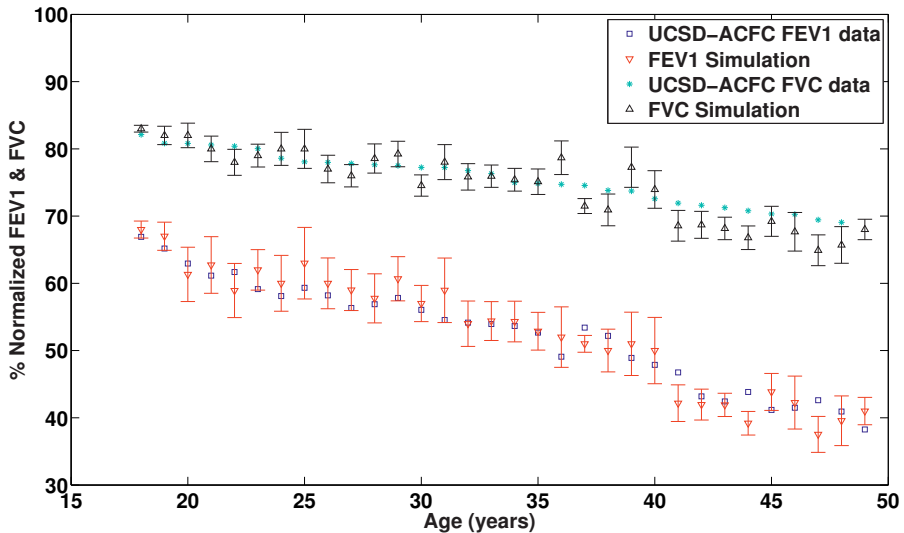


Figure 6. Predictions from the airflow and physiological model (lines) versus the CF patient data (dots) from University of California San Diego Adult Cystic Fibrosis Center. The x -axis is age in years. The y -axis shows the normalized average FEV1 and FVC. The normalization is based on FEV1 and FVC as a percent of FEV1 and FVC for a healthy lung.

CF patients' FVC data as a function of age. Several interesting parameters were identified, including probability of colonization, mucus volume growth rate, and scarring rate [27]. FVC was calculated as the total volume of the accessible alveoli.

To validate our FEV1 model, we used the lung simulation model proposed by Zarei et al. [27] to predict the FEV1 values from ages 18 to 50. We again used UCSD-ACFC FEV1 and FVC data and predicted the mean FEV1 values. Figure 6 displays both the FEV1 and FVC resulting fit including error bars. The figure depicts the airflow and physiological model predictions versus what is observed on average in the CF patient spirometry data. As exhibited in Figure 6, on average CF patients begin with almost 90% FVC and 70% FEV1 of a healthy lung at age 18. This value drops to almost 65% FVC and 40% FEV1 by age 50. The model mean squared errors are 1.05×10^{-4} for FEV1 and 7.9×10^{-5} for FVC predictions, indicating that our model matches both the average FVC and FEV1 data from the patient registry.

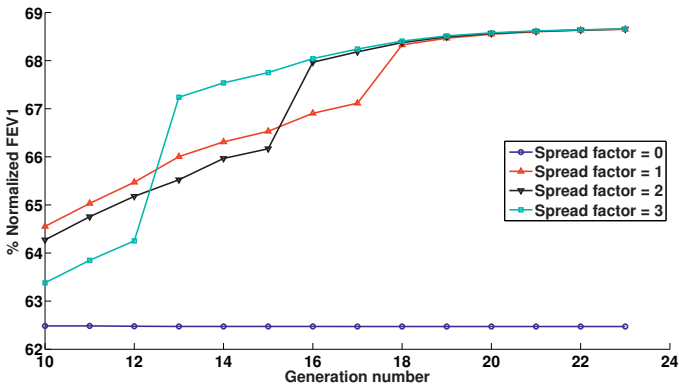
6.2 Mucus redistribution

Initially, we consider only scenarios in which bronchioles are either completely healthy and open, or completely filled with mucus and obstructed. We then consider varying the volume fraction of the blocked tubes with mucus, for a constant FVC value. We held FVC constant by using the same number of accessible alveoli at each experiment.

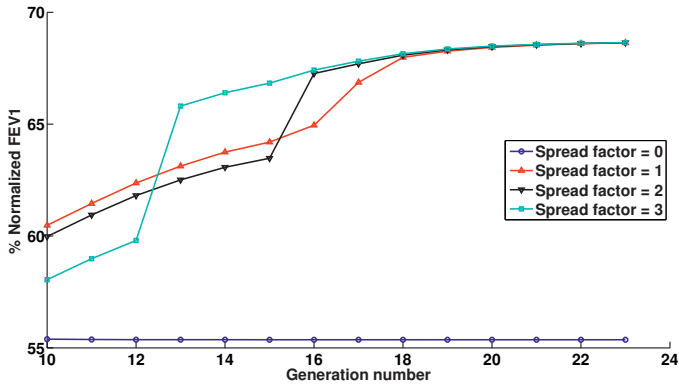
Figure 7(a)–(c) illustrates this situation for FVC values of 90%, 80%, and 70%, respectively.² For each FVC value, bronchioles in one generation were filled until the percent of accessible alveoli matched the chosen FVC value. The different curves in each panel refer to how localized the filling algorithm was. At spread factor 0, siblings of filled bronchioles are preferentially filled. Thus, at this spread factor, we try to fill as local a pocket as possible. At spread factor 1, a sibling of a filled bronchiole is never filled, although first cousins are preferentially filled. Similarly, at spread factor two, siblings and first cousins of filled bronchioles are never filled but second cousins are preferentially filled. This has been illustrated in Figure 8.

As seen in Figure 7(a)–(c), different mucus distributions with different FEV1 values can produce the same FVC depending on the way obstructed airways are distributed in the respiratory system. This is clearly illustrated in this figure, where as the location of obstructed bronchioles moves through the different generations, and the FVC value remains constant, the FEV1 varies significantly. As we can see, when plugged tubes are one after another in any generation (spread factor = 0), the value of FEV1 is independent of the location of mucus. On the other hand, as the spread factor increases, especially when obstructed tubes are located in larger airways, the FEV1 drops (for spread factors $\neq 0$). This effect changes as we move to smaller airways. For instance, in Figure 7(b), where FVC is 80% of a healthy lung, for generations 12 and higher, as the spread factor increases the FEV1 value also rises. We see the same result in Figure 7(c), where we could only have three spread factor values applied due to an in-

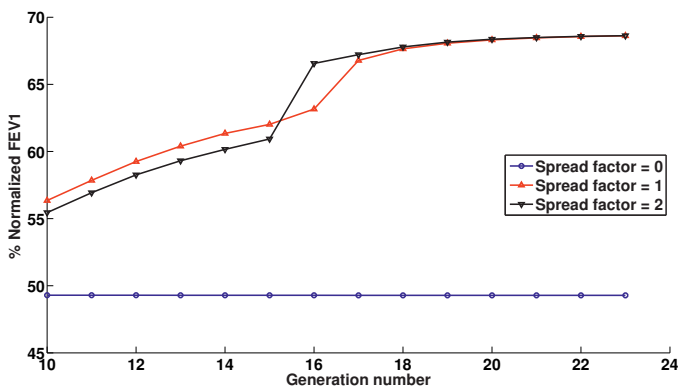
² In Figure 7, bronchioles are either completely open or fully blocked with mucus. For a given FVC (70%, 80%, and 90%), as the location of obstructed bronchioles move to the different generations, FEV1 values change while FVC values stay constant. Each plotted line in these figures refers to a different spread factor. The spread factor indicates the amount of spreading of blocked bronchioles in generation n . Therefore, the corresponding grandparents at generation $n - 2$ can have either 8, 4, 3, 2, or 1 of their grandchildren completely blocked. The higher the spread factor is, the more spread the obstructed tubes are from one another in one generation. Spreading the blocked tubes can have less negative impact on smaller airways compared to larger ones in lower generations.



(a) FEV1 variation versus mucus position at FVC= 90%.



(b) FEV1 variation versus mucus position at FVC= 80%.



(c) FEV1 variation versus mucus position at FVC= 70%.

Figure 7. Variation of FEV1 by the position of blocked bronchioles.

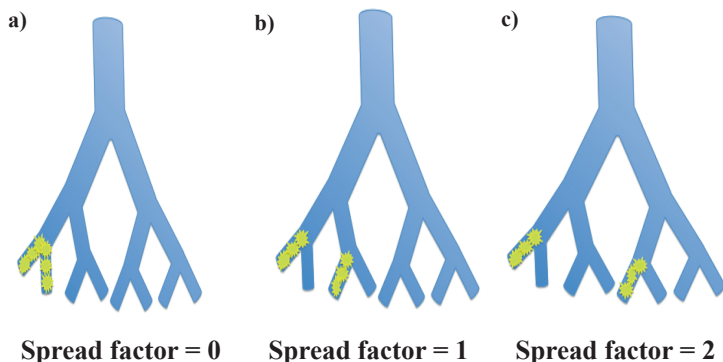


Figure 8. Mucus spread factor illustration used in infection propagation algorithm. At spread factor zero, bronchioles are filled as local a pocket as possible. For spread factor 1, a bronchiole and its first cousins are preferentially filled. Analogously, at spread factor two, a bronchiole and its second cousin are filled.

crease in the number of blocked bronchioles. Based on these figures, we can conclude that if there are completely blocked tubes at larger airways in lower generations, their negative impact can be reduced if they do not spread. On the other hand, if completely obstructed airways are mostly located in smaller airways, FEV1 values will improve if FVC reduction is due to vast spread of infection rather than being positioned locally.

In addition, Figure 7 (a)–(c) shows that if bronchioles become blocked in lower generations closer to the trachea, they will cause a rapid reduction in FEV1 compared to higher generations. This is mostly due to the fact that as a parent bronchiole is completely blocked it will block all tubes distal to it, which in turn reduces the airflow rate or FEV1.

We now consider a more complicated scenario including bronchioles that are partially filled with mucus. We base the scenario on an arbitrarily chosen FVC value of 80% obtained by completely blocking bronchioles in generation 14. We then examine the FEV1 values that result as the rest of the lung is becoming partially filled with a certain percentage of mucus as we go from top to bottom of Table 2. Furthermore, as we read the table from left to right, the volume fraction of mucus in those partially filled tubes increases. For instance, the first cell depicts a case where 10% of the lung with an FVC value of 80% is partially filled with mucus and the volume fraction of mucus is 10% of the total corresponding bronchiole volume.

According to Table 2, FEV1 values decline faster as we go from left to right than from top to bottom. This indicates that if the same amount of

Mucus spread	Mucus concentration			
	10%	20%	30%	40%
10%	64.50	61.16	59.25	57.48
20%	61.26	59.41	56.73	53.96
30%	60.94	58.09	54.00	50.69
40%	59.83	56.04	51.94	46.11

Table 2. Effects of mucus distribution and concentration on FEV1 (FVC = 80).

mucus is spread out as opposed to being concentrated in one location, it will have less of a negative impact on reducing the FEV1 value. We have set our table in a way that as the row and column of a cell are interchanged, the result is the same amount of mucus. For example, if we consider the last entry in the first row, it has the same total amount of mucus as the last entry in the first column. The FEV1 value is 57.47 when there are 10% partially filled bronchioles with a mucus volume fraction of 40% of their volumes. On the other hand, when there are tubes 40% partially filled mucus with 10% mucus volume fraction we obtain an FEV1 value of 59.8, which is relatively higher than the FEV1 value in the previous case. Therefore, according to our result, FEV1 decreases when either the concentration of mucus or mucus spreading increases. On the other hand, given the same amount of mucus, FEV1 decreases at a lower rate as mucus spreads instead of becoming more concentrated. Using this analysis we can say that by using Vest Therapy (High Frequency Chest Wall Oscillation), the FEV1 value improves since it pushes out the mucus located in the lower generation as sputum and it helps to dissipate the mucus in upper generations.

Therefore, physicians may notice that the FEV1 improvement after using Vest Therapy is not solely due to the mucus eradication by mini coughs that dislodge mucus from airway walls, but also to the spreading of mucus in smaller airways located at higher generations.

7 Conclusions

Due to the fact that transport and deposition of therapeutic or pollutant particles in a lung rely on the way in which they are transported, understanding airflow structure–function relationships is an important aspect of both treating and preventing any type of lung obstruction disease including cystic

fibrosis. In this research we described a respiratory airflow model that was used to predict the FEV1 value of CF patients by considering their lung airway flow dynamics. First, we proved that the all-laminar flow assumption that has been widely applied in numerous research studies is an unreasonable assumption. We were able to implement a series of mathematical relationships between turbulent, transitional, and laminar flow, pressure drop and resistance that we used to calculate FEV1 values for any given mucus distribution in a CF lung. Most importantly, the model is a computationally affordable system that calculates the rate of airflow for all 23 airway generations which cover the entire lung airways.

The airflow model was able to calculate the FEV1 in the case of airway obstructions. Based on our Reynolds number calculation, we determined which generations carry turbulent, transitional, or laminar flow. This can be useful in studies that deal with particle deliveries in respiratory systems. Furthermore, our mucus distribution study cases revealed clinically useful information. For a given FVC, we can have different combinations of airflow resistance and FEV1 values. This indicates the importance of FEV1 values compared to those of FVC. Per our research study, if obstruction occurs in lower generation airways (larger diameter), FEV1 values decline at a higher rate as compared to the rate for upper generations becoming blocked. In addition, according to Figure 7 (a)–(c), if the completely blocked bronchioles are located in larger airways, it is better to avoid dissipating the mucus. This finding was totally opposite to when completely obstructed bronchioles were located in smaller airways. On the other hand, based on our results, FEV1 values can improve if we distribute the partially filled bronchioles in a CF lung, irrespective of whether they are in upper or lower generations. This can be done by Vest Therapy (High Frequency Chest Wall Oscillation) or Postural Drainage and Percussion, also known as chest physical therapy.

For our next step we are developing a GUI (graphical user interface) implementation of our model where physicians can enter patients' FEV1 and FVC values and find the maximum likelihood distribution of mucus in their lungs. This can be used as a tool for selecting the most effective treatment as well as a reference tool to estimate the efficacy of different treatments. Finally, the GUI programming implementations of the model will enable medical doctors to interact with the simulation and tailor their treatment based on contrasts between predicted and observed scenarios.

Acknowledgments. This material is based upon work supported by the National Institutes of Health under grant no. 56586B. The authors wish to acknowledge the helpful comments and suggestions made by Mohammad Abouali, Dr. Douglas J. Conrad, Ben Felts, Carol Hand and James Nulton.

Bibliography

- [1] Anogeianaki, A., Negrev, N. and Ilonidis, G., Contributions of signal analysis to the interpretation of spirometry, *J. Hippokratia*, 11(4) (2007), 187–195.
- [2] Bennett, C. O. and Myers, J. E., *Momentum, Heat, and Mass Transfer*, McGraw-Hill, New York, 1962.
- [3] Calay R. K., Kurujareon, J. and Hold, A. E., Numerical simulation of respiratory flow patterns within human lung, *Respir. Physiol. Neurobiol.*, 130(2) (2011), 201–221.
- [4] Corey, M., Edwards, L., Levison, H. and Knowles, M., Longitudinal analysis of pulmonary function decline in patients with cystic fibrosis, *J. Pediatrics*, 131 (1997), 809–814.
- [5] Edwards, L. J., Modern statistical techniques for the analysis of longitudinal data in biomedical research, *J. Pediatric Pulmonol.*, 30 (2000), 330–344.
- [6] Gatlin, B., Cuicchi, C., Hammersley, J., Olson, D. E., Reddy, R. and Burnside, G., Computation of converging and diverging flow through an asymmetric tubular bifurcation, *ASME FEDSM97*, 3429 (1997), 1–7.
- [7] Gatlin, B., Cuicchi, C., Hammersley, J., Olson, D. E., Reddy, R. and Burnside, G., Particle paths and wall deposition patterns in laminar flow through a bifurcation, *ASME FEDSM97*, 3434 (1997), 1–7.
- [8] Holman, J. P., *Heat Transfer*, McGraw-Hill, New York, 2002.
- [9] Ingram, R. H. and Pedley, T. J., Pressure-flow relationships in the lungs, *Compr. Physiol.*, 18 (2011), 279–285.
- [10] *IUPAC Gold Book, Green Book*, 2nd edn., p. 13, Blackwell Scientific Publications, Oxford, 1996.
- [11] Jaffrin, Y. and Kesic, P., Airway resistance: A fluid mechanical approach, *J. Appl. Physiol.*, 36 (1974), 354–361.
- [12] Kikuchi, Y., Sasaki, H., Sekizawa, K., Aihara, K. and Takishima, T., Force-velocity relationship of expiratory muscles in normal subjects, *J. Appl. Physiol.*, 52(4) (1982), 930–938.

- [13] Konstan, M. et al., Risk factors for rate of decline in forced expiratory volume in one second in children and adolescents with cystic fibrosis, *J. Pediatr.*, 151 (2007), 134–139.
- [14] Kulish, V. V., Lage, J. L., Hsia, C. C. W. and Johnson, R. L., A porous medium model of alveolar gas diffusion, *J. Porous Media*, 2 (2002), 263–275.
- [15] Nowak, N., Kakade, P. P. and Annapragada, A. V., Computational fluid dynamics simulation of airflow and aerosol deposition in human lungs, *Ann. Biomed. Eng.*, 31 (2003), 374–390.
- [16] Paul, C. R., *Fundamentals of Electric Circuit Analysis*, pp. 13–27, John Wiley & Sons, New York, 2001.
- [17] Pedley, T. J. and Drazen, J. M., Aerodynamic theory, *Compr. Physiol.*, 4 (2011), 44–46.
- [18] Pfitzner, J., Poiseuille and his law, *Anaesthesia*, 31(2) (1976), 273–275.
- [19] Reis, A. H., Miguel, A. F. and Aydin, M., Constructal theory of flow architecture of the lungs, *Med. Phys.*, 315 (2004), 1135–1140.
- [20] Serway, R. A., *Physics for Scientists & Engineers*, 4th edn., Saunders College Publishing, Philadelphia, 1996.
- [21] Slutsky, S., Berdine, G. G. and Drazen, J. M., Steady flow in a model of human central airways, *J. Appl. Physiol.: Respirat. Environ. Exercise Physiol.*, 49 (1980), 417–423.
- [22] Suter, S. P. and Skalak, R., The history of Poiseuille’s law, *Ann. Rev. Fluid Mechan.*, 25 (1993), 1–19.
- [23] Tawhai, M. H. and Lin, C. L., Airway gas flow, *Compr. Physiol.*, 1 (2011), 1135–1157.
- [24] Warsi, Z. U. A., *Fluid Dynamics: Theoretical and Computational Approaches*, 2nd edn., Ch. 1, pp. 12–14, CRC Press, Boca Raton, FL, 1999.
- [25] Weibel, E. R., Design of airways and blood vessels considered as branching trees, in: *The Lung: Scientific Foundations*, pp. 711–720, Raven, New York, 1991.
- [26] Wilquem, F. and Degrez, G., Numerical modeling of steady inspiratory air flow through three-generation model of the human central airways, *ASME J. Biomech. Eng.*, 119 (1997), 59–65.

- [27] Zarei, S., Mirtar, A., Rohwer, F., Conrad, D. J., Theilmann, R. J. and Salamon, P., Mucus distribution model in a lung with cystic fibrosis, *Comput. Math. Meth. Med.* (2012), DOI 10.1155/2012/970809.
- [28] Zhao, Y. and Lieber, B. B., Steady inspiratory flow in a model symmetric bifurcation, *ASME J. Biomechan. Eng.*, 116 (1994), 488–496.

Received August 3, 2012; accepted November 27, 2012.

Author information

Sara Zarei, Computational Science Research Center,
San Diego State University, San Diego, CA, USA.
E-mail: szarei@sciences.sdsu.edu

Ali Mirtar, Electrical and Computer Engineering Department,
University of California San Diego, San Diego, CA, USA.
E-mail: amirtar@ucsd.edu

Bjarne Andresen, Niels Bohr Institute,
University of Copenhagen, Copenhagen, Denmark.
E-mail: andresen@nbi.ku.dk

Peter Salamon, Department of Mathematics and Statistics,
San Diego State University, San Diego, CA, USA.
E-mail: salamon@math.sdsu.edu